Growth of $Tl_2Ba_2CuO_{6\pm\delta}$ Single Crystals by the Self-Flux Method

by

Darren Peets

B.Sc., The University of British Columbia, 2000

A THESIS SUBMITTED IN PARTIAL FULFILMENT OF
THE REQUIREMENTS FOR THE DEGREE OF

Master of Science

in

The Faculty of Graduate Studies

(Department of Physics and Astronomy)

We accept this thesis as conforming
to the required standard

The University of British Columbia

August 5, 2002

In presenting this thesis in partial fulfilment of the requirements for an advanced degree at the University of British Columbia, I agree that the Library shall make it freely available for reference and study. I further agree that permission for extensive copying of this thesis for scholarly purposes may be granted by the head of my department or by his or her representatives. It is understood that copying or publication of this thesis for financial gain shall not be allowed without my written permission.

Department of Physics and Astronomy

The University of British Columbia
Vancouver, Canada

Date 2002-08-23

Abstract

Crystals of the overdoped cuprate superconductor $Tl_2Ba_2CuO_{6\pm\delta}$, with T_c's ranging from 5K to 90K, have been grown by a copper-rich self-flux method and characterized by X-ray Diffraction and with a SQUID magnetometer. The as-grown T_c's were several Kelvin wide, the crystals studied were found to be multi-domain, and the c-axis lattice parameter was found to be 23.143(2) Å for a T_c = 5K crystal.

The successful growth of $Tl_2Ba_2CuO_{6\pm\delta}$ hinged on the ability to exclude carbon while containing the thallium oxides.

This study of $Tl_2Ba_2CuO_{6\pm\delta}$, while still in its infancy, has the potential to reveal a great deal about the cuprate superconductors.

Contents

List of Tables

List of Figures

Acknowledgements

I'd like to thank the Academy. I'd like to thank Dr. Ruixing Liang, who offered a phenomenal amount of help over the course of this project, Drs. Doug Bonn and Walter Hardy, who also certainly chipped in a great deal, and NSERC and the CIAR, which helped out in their usual ways. I wish to thank the guys in the lab and my many would-be collaborators for their continued patience as I wrestle with a particularly unfriendly phase diagram, trying to grow some rather unco-operative crystals. Dave, my co-mad-bomber and favourite TI-2201 reference, deserves special mention here, as does the AMPEL Safety Committee, who have done their utmost to confound such recreational activities, after not noticing the deafening explosions and falling debris for almost a full year. Harold the Rubber Chicken is particularly saddened by the Safety Committee's ruling, as it effectively prevents him from performing the job he was molded to do – flying. I'd like to thank my parents, without whom I wouldn't be here today, and gravity for keeping my feet on the ground.

As a wise man once said, "Time flies like an arrow. Fruit flies like a banana." Harold, sadly, does not fly, as mentioned above. May the Scaling Gods look upon you favourably, and may the Safety Committee re-evaluate its cannon policies.

Chapter 1

Introduction

In the sixteen years since the discovery of high-temperature superconductivity[1], a remarkable amount of effort has been applied to understanding these compounds, resulting primarily in a realization that we do not understand them very well. Theorists rely on experimental results to provide insight into the nature of the materials, and experimentalists depend on their collaborators to supply them with decent samples. The complex nature of the compounds involved makes purity, homogeneity and disorder key concerns when preparing samples, and sample quality is arguably the most serious problem in the field.

In the underdoped and optimally-doped regimes (see Figure 1.1), $YBa_2Cu_3O_{6+\delta}$ (YBCO) crystals have been grown with very high purity[2, 3], and several oxygen-ordered phases may be prepared[4, 5], with exceptionally low disorder. Many other compounds are studied in this regime, typically with much lower sample quality and far more disorder. With most experimental superconductivity research having been focussed on this part of the phase diagram, there is a staggeringly large body of data on such compounds. This allows theorists a great deal of latitude when attempting to explain one or two experimental results, but due to issues such as sample quality and the unique limitations of every experiment, this body of data is sufficiently self-contradictory that theorists cannot fit all data.

In stark contrast to this situation, the overdoped side of the phase diagram has been very poorly studied. Only a handful of compounds are known which can be overdoped to any significant degree, and crystals of these are seldom grown, rarely
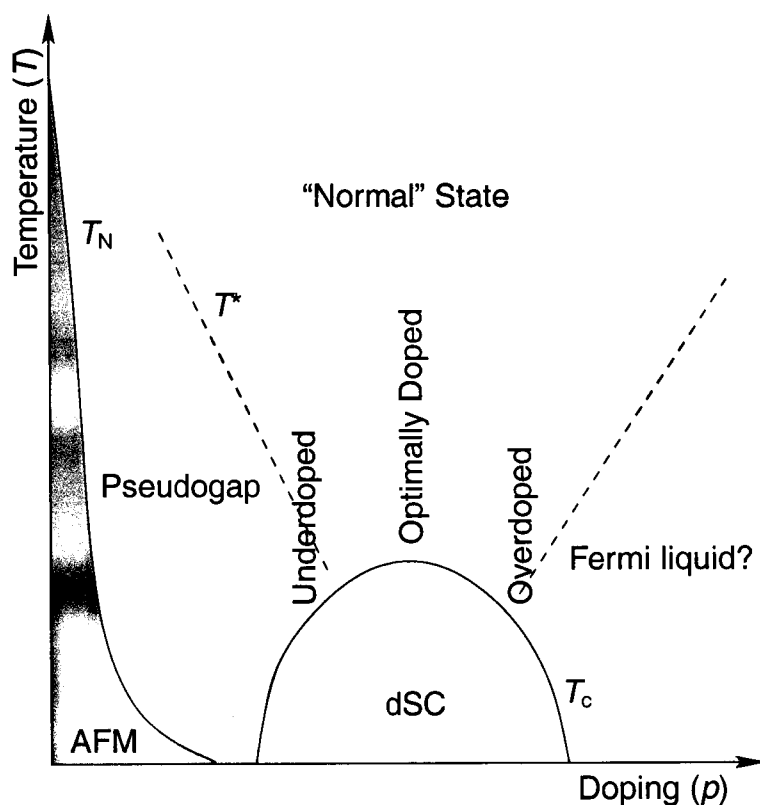
Figure 1.1: Generic cuprate phase diagram. The undoped parent compound is an antiferromagnetic Mott insulator (AFM on the diagram), but hole doping (p) rapidly kills this phase, replacing it with d-wave superconductivity (dSC). The "normal state" above optimal doping seems to have a linear resistivity ($\rho \sim T^1$), and might be satisfactorily modelled by Marginal Fermi Liquid theory, the pseudogap state at lower doping remains poorly understood despite considerable theoretical work, and the overdoped regime might have a Fermi liquid normal state, although there is insufficient evidence to draw a firm conclusion. The grey area at the AFM-dSC boundary has been poorly studied except in LSCO, and may exhibit rich internal structure.

studied, and have not typically been prepared as successfully as the underdoped compounds.

The reason for this is simple: with the exception of $La_{2-x}Sr_xCuO_4$ (LSCO), the compounds which can be heavily overdoped contain either mercury or thallium, both of which are extremely toxic and are volatile in the growth conditions. Most crystal growers avoid them in favour of easier-to-handle alternatives. With few

samples available, and with experimentalists cognizant of the fact that the available samples contain particularly poisonous ingredients, relatively little research has been done on these compounds. The exception, LSCO, is cation-doped and intrinsicly disordered. It exhibits features not observed in other cuprates, such as spin glass phases and a notch in the T_c vs. doping curve apparently due to stripes, and it is unclear whether data taken on LSCO can be considered representative of the cuprate superconductors. LSCO can, however, be overdoped to $T_c = 0$.

With poor samples being used in the few experiments being performed, results on overdoped compounds are particularly open to question, and the lack of experimental work has permitted very little theoretical work to be done. If the overdoped regime's normal state is a close approximation to a Fermi liquid, as most researchers in the field believe, this would make studies of the overdoped regime important – Fermi liquids are well understood, while the normal states in the underdoped regime are not, so there might be an opportunity to understand the mechanisms leading to superconductivity on the overdoped side, possibly deriving the superconductivity from first principles. There is, however, a lack of evidence for this picture, and the normal state in the overdoped regime may be a new state of matter, or may even exhibit several new states of matter. This potential for new physics is still more exciting.

Fermi surface mapping techniques such as cyclotron resonance and de Haas-van Alphen oscillations must be applied at low temperatures, and in the normal state to avoid the gap, requiring either a very low T_c or a very low H_{c2}. These techniques have not been successfully applied to strongly-underdoped compounds, due to their short mean free paths, but strongly-overdoped $Tl_2Ba_2CuO_{6\pm\delta}$ might be more conducive to such measurements. All Fermi surface data thus far has come from ARPES, which can only probe a sample's surface, and is thus highly susceptible to surface states. An astonishing array of other techniques which have

been applied to underdoped compounds have not been tried on the overdoped side, primarily due to a dearth of samples.
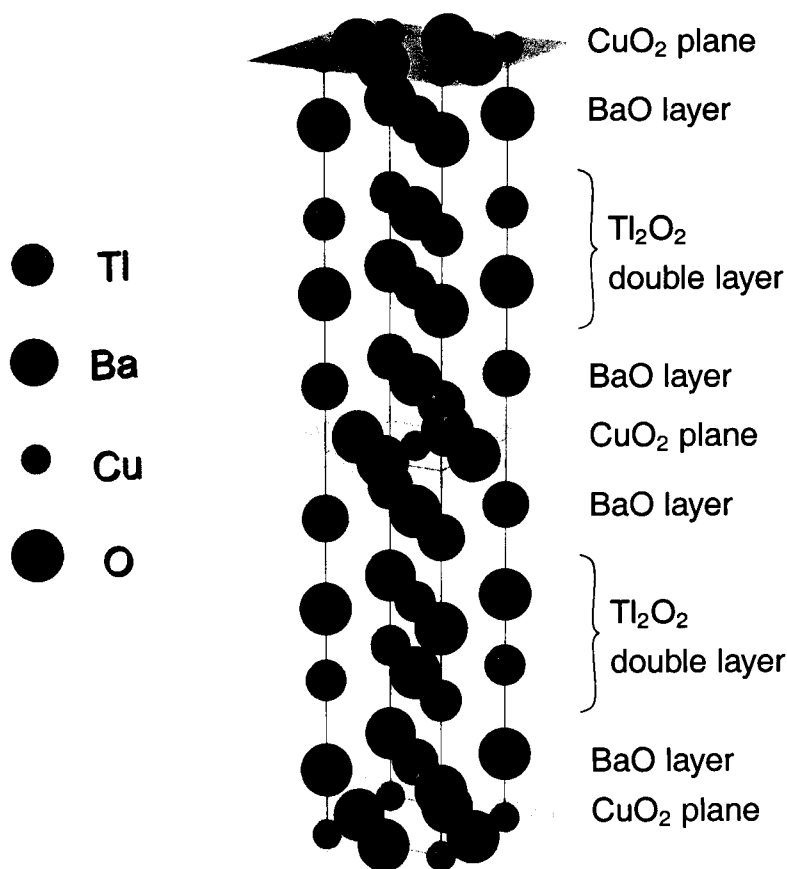
1.1 $Tl_2Ba_2CuO_{6\pm\delta}$

The Hg-Ba-, Bi-Sr- and Tl-Ba-Ca-Cu-O[6] systems have single-layer overdoped members of which crystals can be grown, the "2201" (Tl:Ba:Ca:Cu = 2:2:0:1)) compounds ($Tl_2Ba_2CuO_{6\pm\delta}$ and $Bi_2Sr_2CuO_{6\pm\delta}$) and Hg-1201 ($HgBa_2CuO_{5-x}$). These have simpler crystal structures than almost any of the underdoped compounds and have strictly planar CuO_2 layers, both of which aid data analysis and the former of which improves the odds of preparing homogeneous samples. These compounds are overdoped when stoichiometric. Bi-2201 is extremely two-dimensional, while Tl-2201 is one of the most three-dimensional cuprates – this makes Tl-2201 easier to study with microwaves. We chose the thallium compound over the mercury one for its lower toxicity, its accordingly less-stringent safety considerations, and the accessibility of information on previous work. Hg-1201 has a defect whereby Cu substitutes for Hg; a similar defect may exist in Tl-2201, but there is evidence that it can be controlled in ceramic samples.

Tl-1201 ($TlBa_2CuO_{5-x}$) also exists, but crystals of it have not been grown, and it is prepared at very high pressures.

The crystal structure of $Tl_2Ba_2CuO_{6\pm\delta}$ (Tl-2201) is shown in Figure 1.2. Consecutive CuO_2 planes are shifted by ($\frac{1}{2}$ $\frac{1}{2}$ 0), but are otherwise equivalent.

The oxygen content is not believed to vary significantly from 6.00 ($\delta = 0$), but only relative oxygen contents have ever been directly measured. What is known for certain is that a very small change in oxygen content causes a massive change in T_c – the difference between optimal doping and $T_c = 0$ corresponds to a change in δ of roughly 0.09[7, 8]. For comparison, $YBa_2Cu_3O_{6+\delta}$ first superconducts at

Figure 1.2: Unit cell of $Tl_2Ba_2CuO_{6\pm\delta}$.

$O_{6.35}$ and reaches optimal doping at $O_{6.92}$.

All oxygen nonstoichiometry in Tl-2201 is believed to occur in the TlO double layer, the farthest point from the CuO_2 planes. For dopings $\delta > 0$, the excess oxygen is thought to occupy interstitial sites in the tetrahedral holes between thallium atoms[8–10]. These results, however, are far from convincing, as they come from fitting to powder X-ray and neutron diffraction data and do not allow for the possibilities of substitution of CO for Tl, thallium vacancies, or in one case, cation substitution. In the former scenario, the CO's oxygen atom would likely occupy the interstitial site, but with a very different effect on doping.

One drawback to $Tl_2Ba_2CuO_{6\pm\delta}$ is that it is believed to exist in two phases, orthorhombic and tetragonal, which may be chemically distinct. The former has the

stoichiometric formula $Tl_2Ba_2CuO_{6\pm\delta}$, and has a rhombic CuO_2 plaquette instead of square; to our knowledge, all crystals grown thus far have been tetragonal. This version may have the chemical formula $Tl_{1.85}Ba_2Cu_{1.15}O_{6\pm\delta}$, with an apparent $\sim$15% excess of Cu substituting for Tl[11, 12]. Cation doping typically introduces a great deal of disorder, so we hope to grow the orthorhombic version if possible. If cation substitution is unavoidable, we can take solace in the fact that the cation doping is located, again, at the farthest point from the CuO_2 planes, where it will result in the weakest quasiparticle scattering in the planes. It must be noted that there are doubts as to whether the orthorhombic version of the compound superconducts at all.

Tetragonal Tl-2201 is known to superconduct at temperatures as high as 90 K, with reports of T_c's as high as $110 - 115$ K[10, 13, 14]. These latter crystals, however, grew during attempts to grow $Tl_2Ba_2CaCu_2O_{8+x}$, which superconducts around 115 K. While X-ray diffraction (XRD) scans found at least a few surface layers of Tl-2201, it is likely that intergrowth of calcium-containing layers (Tl-2212) was responsible for the elevated transition temperature. Orthorhombic ceramic samples have been observed to superconduct as well, but it wasn't clear whether this superconductivity was due to the orthorhombic phase itself or due to granular superconductivity of tetragonal phase regions.

1.2   Tl-Ba-Cu Oxide Phase Diagrams

Before a discussion on the relevant phase diagrams can be embarked upon, it is important to introduce some concepts and terminology relevant to phase diagrams. The Gibbs Phase Rule,

$$D = C - P + N, \tag{1.1}$$

indicates how many *Degrees* of freedom there are where *P* phases coexist in a
C-component system with *N* non-compositional variables. For instance, a one-
component system wherein pressure and temperature can change can have three
phases coexisting, but with no degrees of freedom – they can only coexist at a
single point (the triple point of water is such a point). When three components
are present but pressure is irrelevant, many types of region are possible, from
points where four phases coexist to regions where a single phase exists at different
temperatures and compositions. This is the case for the Tl-Ba-Cu oxide system.
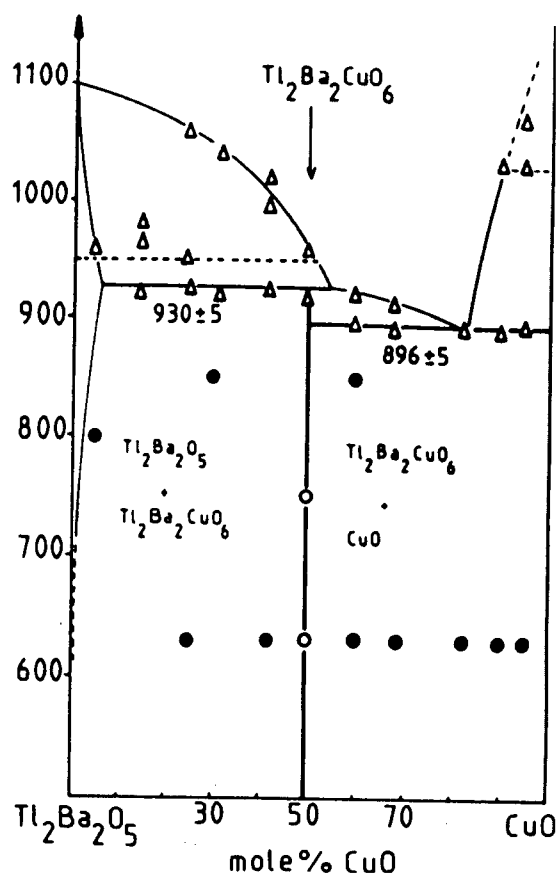
Figure 1.3: A slice through the Tl-Ba-Cu oxide phase diagram, showing a region
where $Tl_2Ba_2CuO_{6\pm\delta}$ is the primary phase, from [15]. The vertical axis
is temperature in °C. The symbols refer to how the points were deter-
mined: $\triangle$ by differential thermal analysis, and $\circ$ and $\bullet$ were single- and
multi-phase regions respectively, as measured by XRD.

Like many of the cuprate superconductors, $Tl_2Ba_2CuO_{6\pm\delta}$ melts incongruently,

at a "peritectic point." Instead of melting into a liquid with identical composition to the solid, as would water or acetone, Tl-2201 melts into a solid phase and a liquid phase, with compositions different from the original solid phase. This makes controlling the inverse process, used in crystal growth, far more challenging. A peritectic point may be readily observed in Figure 1.3, by following the $Tl_2Ba_2CuO_{6\pm\delta}$ composition up to 930°C, where it decomposes.

Another concept which must be introduced is the "liquidus line," a curve below which a solid phase begins to coexist with the liquid. There are three examples in Figure 1.3, the most relevant being the one between 55 and 72 mol% CuO. When the liquid phase is cooled below this line, phase separation occurs, with a solid phase settling out. The compositions of the two phases follow the boundaries of a forbidden dome as the mixture is cooled further. In the case of the liquidus line of interest in this study, a "eutectic point" is reached, where the two liquidus curves meet in a minimum. At this lowest-melting composition, the liquid phase freezes directly into two intimately mixed solid phases, with no interceding phase separation regime. The example is at 72 mol% CuO and 896°C. The constant-temperature line passing through this point has only one degree of freedom – composition – and marks the coexistence of two solid phases with the liquid. This quasi-binary phase diagram does not include a point with four phases and no degrees of freedom.

The thallium oxide stable at ambient conditions is Tl_2O_3, which is also the only thallium oxide available from chemical suppliers. It decomposes completely below 875°C (starting below 500°C) into Tl_2O liquid and O_2 gas[16]. The Tl_2O thus formed has a significant vapour pressure at temperatures as low as 550°C, so it is gradually lost from any open system near growth temperatures ($\sim$950°C). Aside from the obvious chemical concerns about maintaining a stable position in the phase diagram, this gaseous thallium oxide is a serious health concern.

One difficulty in working on $Tl_2Ba_2CuO_{6\pm\delta}$ is the dearth of phase diagrams. The

almost total lack of phase diagrams is both an artifact and a cause of the scarcity of chemical and materials work on this system. The determination of a phase diagram is also strongly hindered by the thallium's vapour pressure.
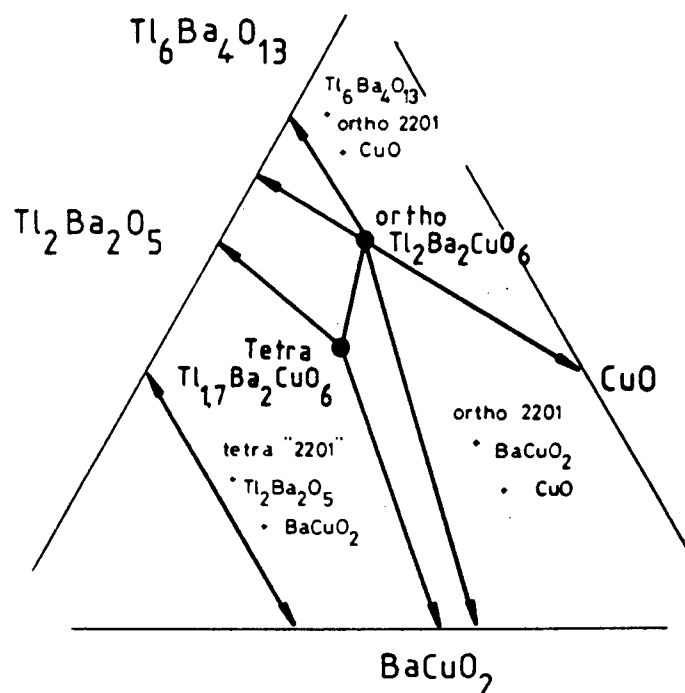
Figure 1.4: A detail of the Tl-Ba-Cu oxide phase diagram in the vicinity of the Tl-2201 phase, under 1 atm O_2. From [15].

The only two (partial) phase diagrams of which we are aware are shown in Figures 1.3 and 1.4. The former is a quasi-binary phase diagram between $Tl_2Ba_2O_5$ and CuO, and the latter is a detail of the area around Tl-2201, as inferred from the known or suspected solid phases in the Tl-Ba-Cu oxide system.

The keys to growing high-quality crystals by a self-flux method (Section 1.3.2) are finding a region in the phase diagram where the desired compound is the primary phase (first phase to crystallize from a melt on cooling) and working in the most favourable (usually the most dilute) corner of that region. The phase diagram (Figure 1.3) suggests that such a region exists between about 55 and 72 mol% CuO. Figure 1.4 depicts results inferred from a study in which only the thallium

content was varied, the conclusion of that study being that the tetragonal phase is thallium-deficient. The tie lines were inferred based on the known phases present in the system.

Groups who have succeeded in growing crystals of $Tl_2Ba_2CuO_{6\pm\delta}$ typically used unoptimized compositions which happened to work for them more often than not, but cannot necessarily be reproduced by other groups. Thallium contents are reported for the mixture of powders initially placed in the crucible, but the (time-varying) thallium content during crystal growth is generally not known. The upshot of all this is that copying other crystal growers' compositions is not only of little benefit, but stands an excellent chance of failure unless the thallium losses can be similarly reproduced.

We chose to base this work on Figure 1.3, for lack of an alternative.

1.3 Flux Growth Techniques

Crystals may be grown in several different manners. In some methods, such as Czochralski growth, precursors are mixed in a near-stoichiometric ratio and melted, then completely (or nearly completely) crystallized. Deviations from exact stoichiometry are amplified as the crystal grows, so off-stoichiometry variants of these techniques require either very large quantities of the reagents that they be replenished, to keep the composition approximately stable. Due to the large crystal volumes involved, such growth techniques can take a long time. In flux or solution growth techniques, the goal is not to crystallize the entire mixture, but to grow a few, smaller crystals, using a melt or solution which has whatever composition gives the best results. An example of the former is the growth of silicon crystals for semiconductor applications, while an example of the latter is the formation of sugar crystals in a supersaturated water solution. The distinction between flux and

solution methods is that the flux is a solid at room temperature.

In thallium systems, stoichiometric techniques such as seeded melt-growth and crystal-pulling, which make large, industrially-useful crystals, are effectively defeated by the thallium's high vapour pressure. Flux methods, which make smaller single crystals suitable for fundamental research, are made more difficult, but thallium losses can be mitigated through time constraints, compositional adjustments, or physical barriers.

1.3.1 KCl Flux

Shortly after the discovery of $Tl_2Ba_2CuO_{6\pm\delta}$, it was found that the compound could be crystallized in a KCl flux[17]. A mixture of $1-10$ % Tl-2201 by mass was added to KCl, loaded into a gold crucible with a gold lid, and cooled from 920°C to 750°C at $1-10$ $\frac{°C}{h}$ in a slight temperature gradient.

Crystals grown in this manner were a few mm^2. While the use of a water-soluble flux made it easy to extract crystals without flux on them, water reacts with the surfaces of many of the cuprate superconductors, including $Tl_2Ba_2CuO_{6\pm\delta}$ – this method of extrication from the KCl flux would have seriously damaged the crystals. In addition, any flux inclusions within the crystal would not have been removed by the water. It is also worth noting that KCl itself is volatile at growth temperatures, and would have added its partial pressure to that of the thallium oxide, making the reaction mixture more difficult to contain and its composition more difficult to control.

A far more serious concern is infiltration of K and Cl into the crystal. If these replaced ions in the crystal (for example, K may substitute for Ba), they would alter the crystal's doping and add disorder, likely depressing T_c.

While using this sort of a flux growth technique produces sizable crystals which do *appear* to be very high quality, their use in fundamental research would be

extremely questionable, particularly for surface-sensitive probes.

1.3.2 Self-flux

The problems mentioned above are largely solved by the self-flux technique, which uses components of the compound as flux, thus the atoms present in the desired crystal, here thallium, barium, copper, and oxygen, are the only species present inside the crucible. A handful of groups have succeeded in growing $Tl_2Ba_2CuO_{6\pm\delta}$ this way.

In its most basic form, the self-flux method involves choosing a composition of precursors, loading this mixture into a crucible, melting it, cooling it through the temperature range where crystals form, and extracting the crystals. Thallium oxides, being volatile, usually require that the crucible have a lid to help suppress the diffusion of Tl_2O vapours. The techniques summarized in Table 1.1 involved little more than this.

Table 1.1: Other groups' growth parameters. It is not clear from Kolesnikov's papers whether he used inverted crucibles as lids or used no lids at all. This difference would have had very little impact on his results.

Group	Tl:Ba:Cu	Crucible	Lid	Temperature Program
Torardi[18]	$1:1:1$	Au	Au	"Slow cooling"
Liu[19]	$1:1:\frac{3}{2}\sim2$	Al_2O_3	Au	$910 - 870°C$ in 40h
Tyler[11]	$1.34:1:\frac{3}{2}$	Al_2O_3	Au	$892\sim895°C$, 3 min.
Kolesnikov[14]	$2:2:1$	Al_2O_3	Unclear	$950°C, -5\frac{°C}{h}$
Kolesnikov[10]	$1:1:1$	YSZ	Unclear	$950°C$, 30 min.
Hasegawa[20]	$1:1:1$	Au	Au	10h@915°C, 10h to 895°C
Hasegawa[21]	$1:\frac{5}{4}:1$	Au	Au	10h@920°C, 57h to 880°C

All groups used Tl_2O_3, BaO_2 (barium peroxide) and CuO as ingredients, but each group used its own starting composition and temperature program. It is worth noting that groups preparing powders and ceramics often prefer more complicated precursors, such as $BaCuO_2$, $Tl_2Ba_2O_5$, or any of the many other thallium barium

$TlO_{\frac{3}{2}}$

$Tl_6Ba_4O_{13}$

$Tl_2Ba_2O_5$

$Tl_2Ba_2O_2$

$Tl_2Ba_2CuO_{6\pm\delta}$[14]

[11]

[19]

[10, 13, 18, 20]

[21]

$Tl_{1.7}Ba_2Cu_{1+x}O_{6\pm\delta}$
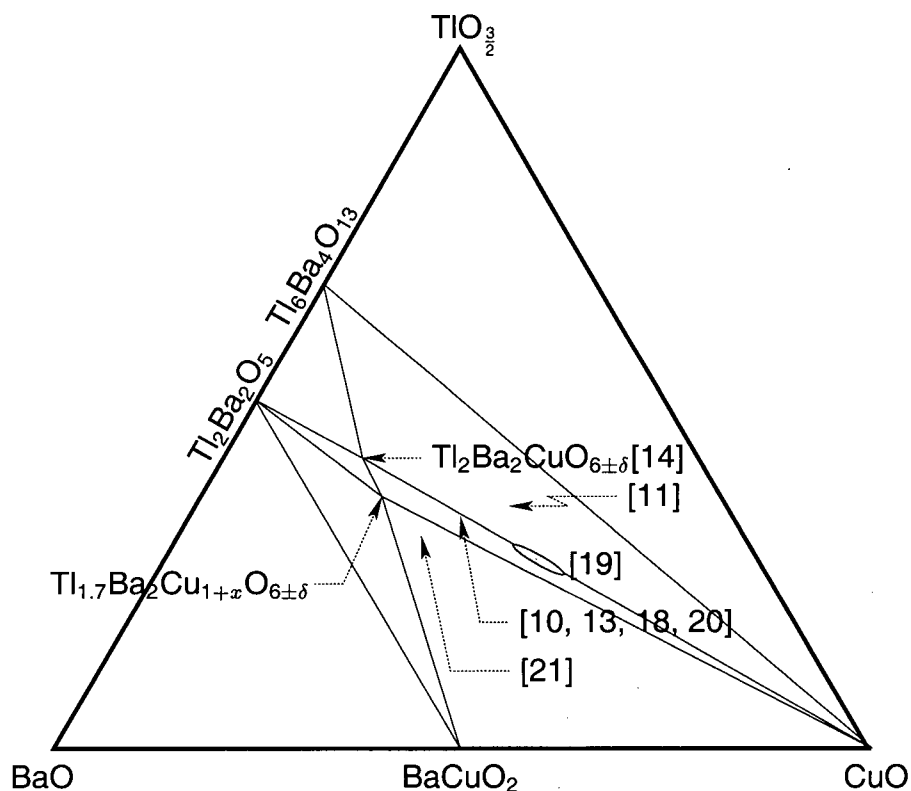
BaO $\qquad$ $BaCuO_2$ $\qquad$ CuO

Figure 1.5: Other groups' growth parameters – phase diagram. Tie lines must not be taken literally, and the actual composition of the tetrahedral 2201 compound is open to debate. This phase diagram is incomplete – known omissions include several thallium barium oxides. Due to thallium loss, most of these compositions drifted significantly both before and during growth.

oxides[22–24].

While using thallium barium oxides can make the thallium less volatile before growth, some thallium evaporates when forming the compounds in the first place, so there is not necessarily a benefit from this technique. Additionally, grinding of highly-toxic thallium-containing powders is required, so this is inconvenient.

Barium peroxide is used in place of more-commonly available $BaCO_3$ to reduce contamination from CO_2, which is a problem because of the necessity of using a closed system. Unfortunately, BaO_2 is difficult to make and decomposes to $BaCO_3$ in air, so it cannot easily be produced or maintained in high purity. It is thus only

available in technical grade ($\sim$95%), and contains such impurities as iron, calcium and alkalis – the use of BaO_2 can introduce significant concentrations of impurity atoms into the melt. Barium nitrate, $Ba(NO_3)_2$, is not considered because it violently evolves extremely corrosive NO_2 gas at its melting point, 550°C, and would wreak havoc with both the other reactants and the apparatus.

One disadvantage to the self-flux technique is that extracting the crystals from the flux is no longer as straightforward as simply soaking the crucible in a beaker of water. Several alternative methods have been devised to effect this separation. For heavy-fermion superconductors such as $CeCoIn_5$ and $CeIrIn_5$, which grow from a very soft and low-melting indium flux, it is possible to centrifuge the melt from the crystals before it hardens[25, 26]. In the case of high-purity $YBa_2Cu_3O_{6+\delta}$, the melt is decanted at the end of each growth run by tipping the crucible over[2, 3].

In all self-flux studies of Tl-2201, including the present work, crystals were separated from the melt mechanically, by breaking up the solidified ingot. It is intended that other, less crude, alternatives will be tested once $Tl_2Ba_2CuO_{6\pm\delta}$ crystals have been successfully and repeatably grown.

1.3.3 Crucibles

As can be seen from Subsection 1.3.1 and Table 1.1, all pre-existing crystals of $Tl_2Ba_2CuO_{6\pm\delta}$ have been grown in crucibles of either alumina (Al_2O_3), gold or YSZ (yttria stabilized zirconia, which is ZrO_2 with a few % Y_2O_3), typically with a gold lid. None of these materials are ideal. Alumina dissolves slowly in BaO-CuO fluxes, contaminating the melt with Al^{3+} ions, which may in turn contaminate any crystals. Aluminum tends to replace copper in the chains in YBCO, so it is unclear whether or to what extent it would displace cations in Tl-2201. Gold reacts with the copper present in these melts, but isn't expected to substitute into the $Tl_2Ba_2CuO_{6\pm\delta}$ matrix to any significant degree, although this has not been tested. YSZ is the worst of the

three − the zirconia reacts with the melt to form solid $BaZrO_3$ (barium zirconate), which clogs up the melt, but yttrium is dissolved. This freed Y^{3+} has the option of either contaminating the Tl-2201 crystals or forming unwanted phases such as $YBa_2Cu_3O_{6+\delta}$.

The solution to crucible corrosion in 123 systems such as $YBa_2Cu_3O_{6+\delta}$ was the use of $BaZrO_3$ crucibles[2, 3], which are inert to BaO-CuO fluxes. These crucibles are also time-consuming and expensive to make with the necessary purity. It is not clear whether $BaZrO_3$ would work in this system, but it certainly warrants testing.

Gold, which is quite soft at growth temperatures, is used as a lid to seal the top of the crucible. In practice, it does not actually seal the crucible, but it acts as a significant barrier to the diffusion of Tl_2O vapours, allowing the thallium to stay in the crucible longer − usually long enough for some crystals to grow. The only closed system in the above table was reported by Hasegawa et al.[21], who encased their sealed gold crucible in alumina cement inside an alumina crucible before firing.

1.4 Oxygen Content Control

As mentioned in Section 1.1, Tl-2201 may be doped by changing its oxygen content. In practice, this means annealing it in a controlled atmosphere. Above some temperature, oxygen atoms in the crystal become mobile, and oxygen may enter or leave the crystal. Above this temperature, a chemical equilibrium is established between the oxygen content of the crystal and the oxygen partial pressure around it, the equilibrium also depending upon the temperature of the system. An oxygen partial pressure and anneal temperature uniquely determine an oxygen content.

$YBa_2Cu_3O_{6+\delta}$ grows strongly underdoped, and oxygen must be added for superconductivity. Since the temperature may be controlled more readily than the

pressure, the pressure is typically fixed at 1 atm of pure O_2, and the annealling temperature is used to set the oxygen content. As-grown $Tl_2Ba_2CuO_{6\pm\delta}$, however, is overdoped, and the addition of oxygen suppresses superconductivity. Frequently, oxygen must still be added to drive T_c toward zero, but lower dopings require oxygen removal. A key concern is how to add or remove oxygen without disturbing the thallium content. Although most doping work has been done on ceramic samples, many of the techniques used should produce similar results on crystalline samples.

The technique used to remove oxygen depends on how much oxygen must be removed. Moderately overdoped crystals can be obtained by annealing under a reduced oxygen partial pressure, attained by mixing oxygen with an inert gas. It appears likely that optimal doping requires a very small oxygen partial pressure, and most groups who claim to have reached optimal doping did so by annealing in a strongly reducing atmosphere, such as H_2 in Ar, to forcibly rip oxygen from their samples. While this method is effective because the freed oxygen reacts to form water, that same reaction is responsible for the technique being unreproducible, because it relies critically upon the (uncontrolled) partial pressure of water:

$$H_2O \rightleftharpoons H_2 + \frac{1}{2}O_2, \tag{1.2}$$

with equilibrium constant

$$K = \frac{P_{H_2}\sqrt{P_{O_2}}}{P_{H_2O}} \quad \text{or} \tag{1.3}$$

$$P_{O_2} = \left[\frac{K}{P_{H_2}}\right]^2 P_{H_2O}^2 \tag{1.4}$$

(note that K has an exponential temperature dependence).

The water partial pressure is usually, but not always, extremely small, and may vary significantly. Because of this, the miniscule oxygen partial pressure may vary

by tens of orders of magnitude within a furnace and over time. The water partial pressure also depends critically on whether a nitrogen trap was used, and can depend on the flow rate of H_2, so there can be enormous variations between groups. H_2/Ar anneals are, therefore, completely unreproducible. This has led the various groups to accuse each other of poor technique or of actually underdoping their samples. H_2/Ar anneals have only proven successful on ceramic samples, where severe surface damage can go unnoticed.

Several groups who grew $Tl_2Ba_2CuO_{6\pm\delta}$ crystals reported difficulties either in reaching extreme dopings[11], or in doping the crystals at all[14], without the crystals beginning to degrade. This could be due to thallium losses, or to $Tl_2Ba_2CuO_{6\pm\delta}$ decomposing.

The only paper which reports on the relationship between oxygen partial pressure, annealing temperature and T_c was [22], which should serve as an adequate rough guide when first annealing samples. It may not, however, prove sufficiently thorough, so we will have to devise our own $P_{O_2}-T-T_c$ phase diagram.

Chapter 2

Experimental

In all growth runs, a mixture of thallium, barium and copper precursors were packed into a small crucible, which was then placed on an alumina tray and sealed. This assembly was inserted into a horizontal tube furnace, the powder was melted, slowly cooled through the growth region, then cooled rapidly to room temperature. Specifics and variations on this method are detailed below.

2.1 Furnace

All steps involving the heating of thallium compounds were performed in a horizontal tube furnace (Thermolyne F79340) with a quartz tube insert. This furnace has a 12" heated length, can accomodate tubes up to 3" in diameter, and is able to store four programs of eight ramps and eight dwells. The temperature is measured with a Platinel-II thermocouple, an inert metal simulation of K-type, which is positioned between the tube and elements at the midpoint of the heated zone.

The main quartz tube is roughly 1 m long, and extends about 20 cm outside each end of the furnace casing. The tube has inner and outer diameters of 74 mm and 70 mm respectively. An inner quartz tube (inner and outer diameters 69 and 65 mm, ~20 cm long) is used to ease moving and centring of the sample within the furnace, and to prevent the sample assembly from scratching or spilling onto the main quartz tube.

Cylindrical firebrick plugs were placed inside the main quartz tube where it exits the furnace. These prevent convection from spreading contaminants to the inlet
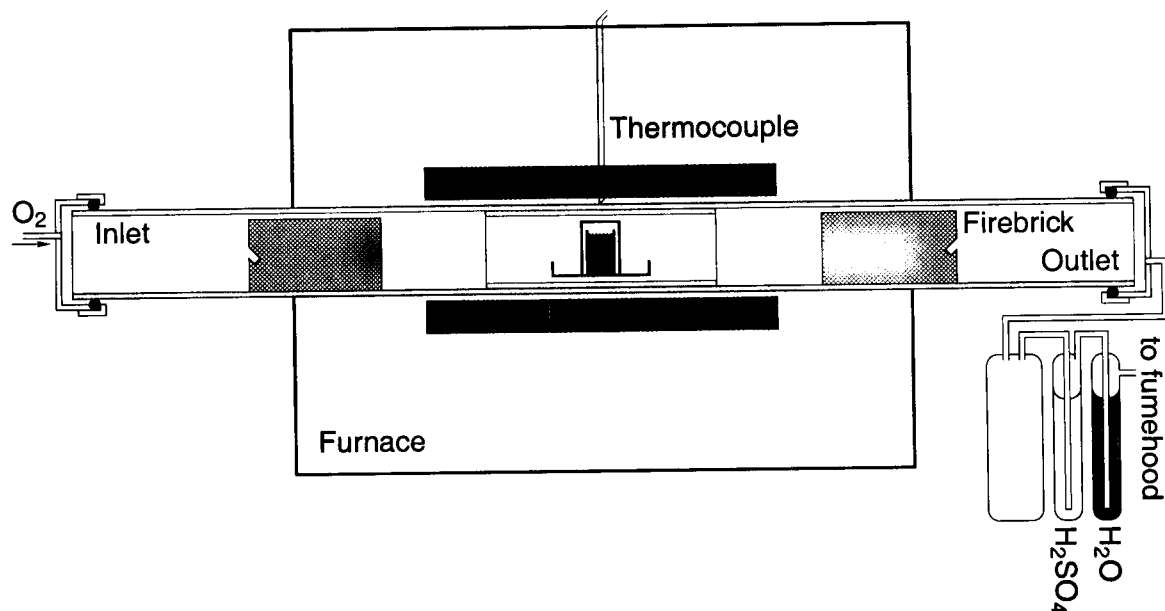
Figure 2.1: Schematic diagram of the furnace and gas handling system. 10% H_2SO_4 is used to scrub any remaining thallium oxides from the air before its release into the fumehood. The region marked "furnace" is almost entirely insulation.

end, keep temperature gradients in check, and prevent the caps on the ends of the furnace from heating up. The airtight aluminum caps rely upon neoprene rubber O-ring seals, which could melt or deform if the aluminum were heated excessively.

The furnace's thermocouple was calibrated against a factory-calibrated R-type thermocouple, which is believed to be accurate to within 1°C. A tray and outer crucible were placed in the furnace to simulate the standard sample assembly, and a third firebrick plug, with a hole along its axis for the thermocouple, was used. To negate any effects due to the presence of the thermocouple, measurements were taken as a function of horizontal position within the furnace, and from both ends. The calibration thermocouple had a reference joint which was held at the ice point.

2.2   Powder Preparation

The chemicals used as precursors were purchased in the best available purity: Tl_2O_3 from Alfa Æsar (99.99 % pure), $BaCO_3$ from Aldrich-APL (99.999 %), and CuO from Alfa Æsar (99.995 %). The BaO_2 used (Fisher Scientific, 96 %) was obtained around 1989, and had partially decomposed into carbonate ($\sim$ 20 %). Once it became clear that carbonate-free BaO_2 would be required, more was purchased from Sigma-Aldrich (97%). As mentioned in Subsection 1.3.2, only technical grade barium peroxide is available, and its use is a significant source of potential impurities. $BaCuO_2$ was prepared from $BaCO_3$ and CuO by calcining at 850°C. The $BaCuO_2$ contained less residual carbonate when the final calcining step was performed in a pure O_2 atmosphere.

Thallium was introduced as late as possible in the process, to minimize the handling of toxic thallium oxides. All masses prior to the introduction of thallium were measured on a Mettler-Toledo AX205 analytical balance, and all masses after the addition of thallium were measured on a Mettler AE163 analytical balance inside a glovebox. Before the latter balance was placed in the glovebox, it was compared against the former, to ensure measurement consistency.

The precursor powders were weighed into a 125 mL plastic (Nalgene) bottle and hand ball-milled for 15-20 minutes, using ZrO_2 balls. 15-20 g of mixed powder were then packed into a small crucible, which was placed on a rectangular alumina tray, covered, and inserted into the furnace. The geometry is shown in Figures 2.2, 2.4 and 2.5 and is described in Section 2.4.

2.3   Crucibles

All crucibles and related parts used in these experiments were 99.8 % pure alumina (Al_2O_3), AD-998, from CoorsTek Ceramics. The smaller crucibles were CN-

10 cylindrical crucibles, the larger crucibles were CN-20's and the trays were CR-32's. While it was observed in Subsection 1.3.3 that using alumina for the inner (smaller) crucible risks contamination of the melt and crystals, alumina was nonetheless chosen as a comparatively common and inexpensive crucible material. Only once the crystal growth technique has been optimized will less-harmful alternatives be tested. It is hoped that a method of separating the flux from the crystals will be found which will also permit the re-use of crucibles.

Alumina may be readily cleaned in dilute acid. Oxides of thallium, copper and barium all either dissolve in acid or precipitate out of solution, depending on the acid used. Both nitric (HNO_3) and sulfuric (H_2SO_4) acids are used for this purpose; sulfuric cleans more slowly, but is non-volatile and thus easier to handle. Both acids may permeate the ceramic, requiring that the alumina be boiled in deionized water for several minutes after cleaning – remnants of acid left in the ceramic can cause it to explode on heating.

2.4 Controlling Tl Losses

Several techniques for impeding thallium losses were tested. This is key to achieving successful and repeatable growth, as gradual loss of one component not only changes one's position in the phase diagram, it does so dynamically – the mixture has time-varying compositions and compositional gradients until the thallium is completely eliminated from the reaction vessel.

2.4.1 Sealing with Salt

Most of our crystal growth runs thus far have employed the salt-sealing method depicted in Figure 2.2. A salt mixture is used to seal the outer crucible to the tray. If this works properly, thallium vapours must either bubble or diffuse through the
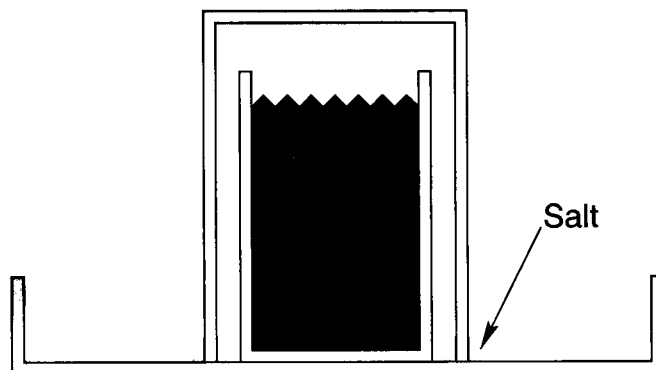
Figure 2.2: Sealing the crucible with salt (side view).

molten salt in order to escape the system.

The chosen salt mixture was 70 % $BaCl_2$ and 30 % KCl. Barium chloride was preferred because barium was already present in the melt. KCl was chosen over the alternative, NaCl, because KCl has a slightly lower vapour pressure. The exact mixture of the two salts was chosen based on the phase diagram in Figure 2.3, to have a melting point around 825°C. By placing the outer crucible initially atop a mound of salt, the oxygen atmosphere was allowed to diffuse into the sealed region around the powders for several hours before the salt fully melts to seal the system. The two constituent salts were dry-mixed by hand using a ceramic mortar and pestle.

Initially, enough salt was added that, as a liquid, it was a few mm deep throughout the tray (roughly 20 g). This resulted in near-perfect sealing, but unfortunately also in contamination of the reaction mixture. The salt had a strong tendency to wet the alumina, so it was able to enter the inner crucible, contaminating the melt with KCl and reacting with CuO to form BaO and unreactive copper chlorides. With the copper oxide almost totally depleted, no copper-containing crystals grew. The salt also escaped onto the inner furnace tube, inflicting serious damage.

Once it became clear that it would be impossible to grow $Tl_2Ba_2CuO_{6\pm\delta}$ crystals in such a lake of salt, the amount of salt was reduced to about 0.4 g, enough to
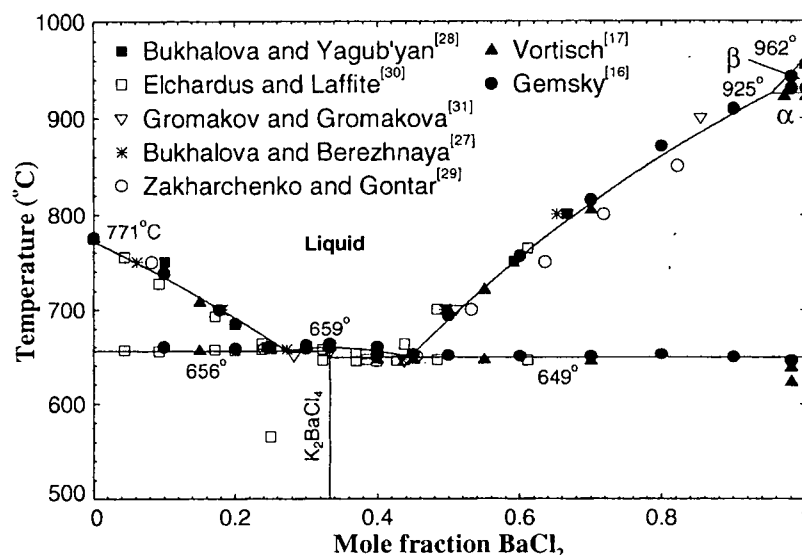
Figure 2.3: KCl-BaCl$_2$ phase diagram, from [27]. The references are from the
source, not this thesis. 70 mol% BaCl$_2$ corresponds to a melting point
of roughly 825°C.

seal the outer crucible but not enough salt to reach the melt. It should be noted

that the finite vapour pressure of KCl near the growth temperature means that

such a salt sealing system will still contaminate the melt at some level. Also, the

solubility of thallium oxides in KCl, made use of in the KCl flux method described in

Subsection 1.3.1, allows them to dissolve in the salt seal, diffuse under the outer

crucible, and re-evaporate. Because of the very small gap between crucible and

tray, this process is expected to be slow.

2.4.2 Sealing with Gold

As an alternative to salt, we adapted the design for gold. An additional gold lid was

added (see Figure 2.4) to further reduce the diffusion of thallium vapours. While

gold does not melt at growth temperatures, it becomes soft, permitting a decent

seal. In an attempt to further improve sealing, a weight was added and the design

modified, using a large rod of a high-temperature-tolerant alloy (Hastelloy X, from
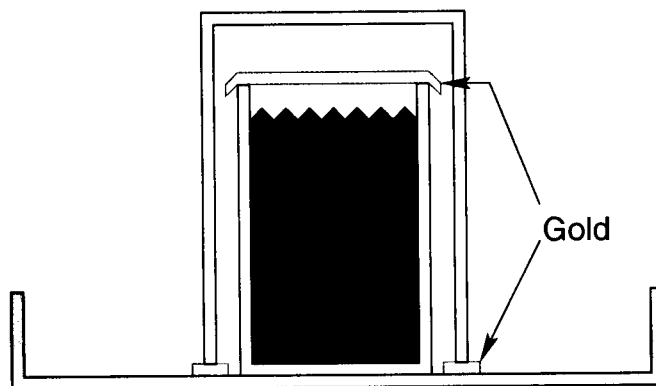
Figure 2.4: Sealing the crucible with gold.

Haynes International), from which a flat side and crucible-sized hole were milled out (see Figure 2.5 for an end view). The rod's mass after these modifications was 915 g.
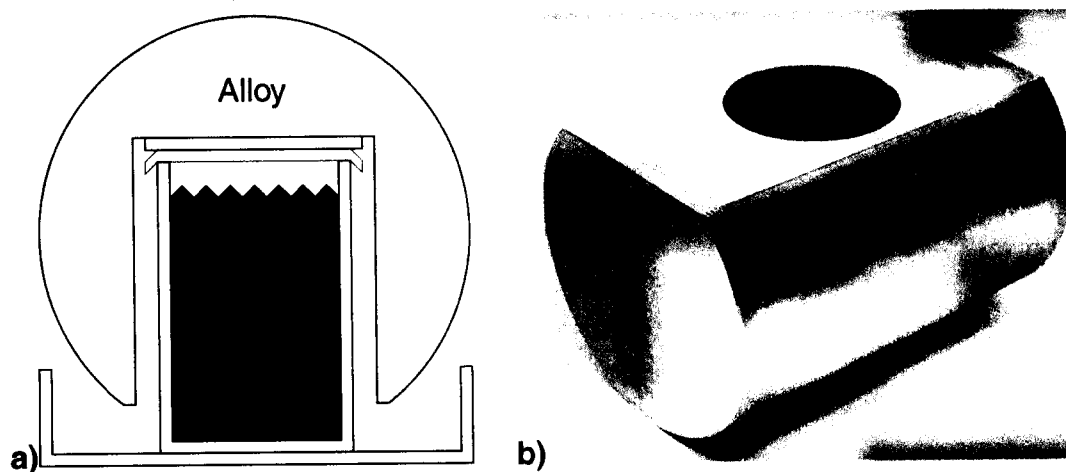

Figure 2.5: Sealing the crucible with extra weight provided by a rod of high-temperature alloy: **a)** Schematic diagram (end view) and **b)** Photograph. An additional Al_2O_3 disk is required to prevent the gold from fusing with the alloy, and the outer crucible is no longer necessary.

Because the weight of the alloy can compress only one gold seal, the outer crucible becomes redundant. In addition, once the gold has softened and the seal has been made, it is virtually certain that the tube's atmosphere will not diffuse into the reaction vessel. The flow of oxygen gas is then only required *for sweeping*

out thallium and CO_2 vapours, so its purity can only have any importance while warming the furnace.

2.5 Oxygen Atmosphere

Medical-grade oxygen gas (Praxair) was used as the atmosphere for all growth runs. Except for cases when purity was less important, such as those mentioned at the end of Subsection 2.4.2, the oxygen was further purified using a liquid nitrogen trap and a system to remove carbon monoxide.

A bubbler was connected to the outlet end of the furnace tube, to indicate the flow rate and prevent the release of thallium. The gas exiting the furnace was first passed through a fine bubbler in 1.8 M sulfuric acid, then through a coarse bubbler in water. Both thallium oxides are soluble in acid[16], so this stage should remove any thallium vapours, preventing their release into the environment. The second bubbler offers a further trap for any unwanted gases or anything evaporating from the acid bubbler. Its larger bubbles ($\sim\frac{1}{2}$ mL) make the flow rate plainly visible, allowing it to be set at a few mL per second. This allows the heated portion of the furnace tube to be purged every 10$\sim$20 minutes.

The pressure in the furnace is kept at 1 atm by the direct connection, through the bubblers, to the atmosphere. The bubblers add 20 $-$ 40 mmH$_2$O or 1.5 $-$ 3 torr over the atmospheric pressure in the lab, but this is largely offset by the building's ferocious ventilation system. Fluctuations due to the weather are typically 10$\sim$15 torr, dwarfing the bubblers' contribution.

2.6 Safety Considerations

Due to the poisonous, dusty and volatile nature of the Tl_2O_3 used, a great effort was made to isolate the thallium from the researchers and equipment. All steps

involving thallium-containing powders were performed in a small room (Brima-combe/AMPEL 244A) with a large fumehood and under significant negative pressure relative to the surrounding laboratories. This room was left locked while unattended, with a large yellow sign warning of the chemicals used within, and a small skull-and-crossbones sticker direcly above the lock.

While some sample- and gas-handling equipment and the furnace controller were left unprotected, these were kept strictly separated from anything that could potentially have thallium powders on it.

Latex gloves were used to handle anything potentially contaminated with thallium. While no face or breathing protection was used, respirators were available both inside and immediately outside the room, in case of spill, fumehood shutdown or similar problem. The procedures used at Cambridge[11] were significantly more stringent – for example, researchers wore cartridge respirators and two layers of gloves at all times, and were subjected to frequent urine tests (thallium was never detected). While there is nothing wrong with this approach, it is unnecessary. If thallium is properly contained and all those using it are well aware of the dangers, it can be handled safely without the need for draconian safety policies. To ensure nothing had been overlooked, the room and setup were inspected by UBC's Health, Safety and Environment department before use.

2.6.1 Storage and Handling of Tl_2O_3

The Tl_2O_3 was stored in an acrylic negative-pressure glovebox with neoprene gloves (Terra Universal), along with an analytical balance and various supplies and handling apparatus. All weighing, mixing and handling of thallium-containing powders were carried out inside the glovebox. The glovebox also contained an empty paint tin for collecting thallium-contaminated refuse. A RubberMaid container was available for transporting samples from the glovebox to the fumehood, where the

furnace was located.

The glovebox was kept at a negative relative pressure to ensure containment of the thallium. This pressure was sustained by a large fan, vented into the fumehood exhaust via 3" ABS sewer pipe. Venting it into the fumehood exhaust was a redundant step, as a HEPA filter separated the fan from the contents of the glovebox.

2.6.2 Furnace and Fumehood

The main portion of the furnace was kept in the fumehood, so that any failure of the furnace would inflict a minimum of contamination upon the room. While the charge loaded into the furnace was usually almost completely assembled inside the glovebox, some steps were sometimes performed in the fumehood. All materials inside the fumehood were handled with latex gloves.

While the furnace was kept in the fumehood, steps were taken to ensure that thallium was not released into the environment. The oxygen exiting the furnace was bubbled through acid and water, as described in Section 2.5, to scrub any thallium oxides from the oxygen. The acid bubbler had a strong-acid indicator, methyl violet (whose pK_a is 0.8), to ensure that any change in pH would be immediately detected.

Nearly all thallium oxide vapours precipitated out on the furnace tube and firebrick plug at the outlet end of the furnace, where the oxygen cooled to room temperature. The airflow helped the inlet end stay clean, so all loading and unloading of samples was performed strictly via the inlet end.

Chapter 3

Results

Despite the time and effort expended on $Tl_2Ba_2CuO_{6\pm\delta}$, crystals of this compound were loathe to grow. This chapter is, therefore, primarily a brief description of what did not work. In attempts to solve various real and perceived problems, vast tracts of parameter space were explored in the process of, for example, testing techniques such as salt sealing, or attempting to locate reaction temperatures in the phase diagram. The results from groping about in parameter space have been largely omitted from this thesis, as they would add only volume. For instance, several Tl : Ba : Cu compositions were tested, including $\frac{4}{3} : \frac{4}{3} : 1$, $\frac{8}{3} : \frac{4}{3} : 1$, $\frac{4}{3} : 1 : \frac{3}{2}$, $\sim \frac{3}{2} : \frac{3}{2} : 1$, $\frac{3}{2} : 1 : 1$, and 1 : 1 : 1, and this variety combined with different cooling rates and thallium losses led to a wide variety in compounds crystallized, including a significant number of thallium barium oxides.

3.1   The Temperature Program

The calibration of the furnace's thermocouple was described in Section 2.1. Despite the size of the furnace tube and the accordingly large convection effects, tests of stability and repeatability at 900°C found that the calibration was accurate ±0.5°C. In practice, the thermal mass of the crucible assembly should damp out most oscillations for the sample, reducing this error significantly.

A variety of furnace programs were tested, most based on the phase diagram in Figure 1.3. They were designed to fully melt the mixture, then cool slowly across the liquidus line, allowing Tl-2201 to form. Rapid cooling was designed to begin

slightly above the eutectic point, to ensure that only crystals of $Tl_2Ba_2CuO_{6\pm\delta}$ would grow.

All furnace programs involved heating the sample at $200-300\frac{°C}{h}$ to 900−950°C, where the program paused for several minutes to allow the sample to equilibrate at that temperature. From that temperature, the now-molten mixture was slowly cooled over 1−30h to 870−920°C, then allowed to cool freely to room temperature (over ∼3 hours). $300\frac{°C}{h}$ is a very rapid heating rate, and is, in fact, double the rate the alumina ceramics are rated for. An example furnace program, used while testing salt sealing, is shown in Figure 3.1.
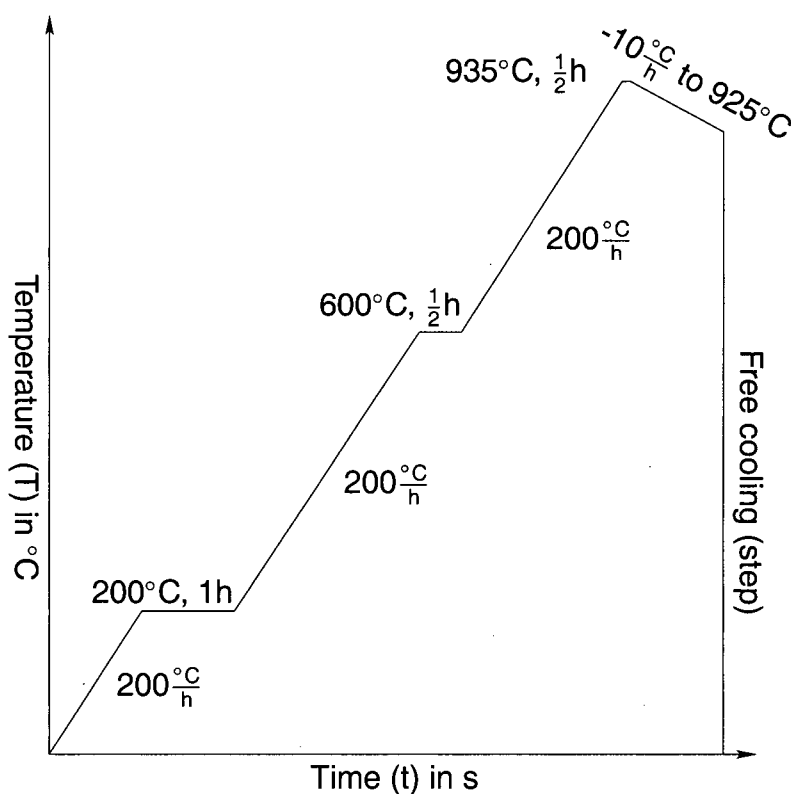

Figure 3.1: An example of a furnace program used with salt sealing. The pause at 200°C allows oxygen to displace other gases and the speedy crystallization portion was used to limit thallium losses. The pause at 600°C and slower (200 instead of $300\frac{°C}{h}$) ramp rates were used in an ultimately counterproductive attempt at allowing the BaO_2 to melt and react with Tl_2O_3, slowly evolving oxygen.

Many of the temperature programs used paused for a few hours while ascending to the growth temperature. Frequently, a pause was added at 200°C to allow the tube to be completely flushed with oxygen, although this was no longer mandatory once the alloy weight was in place. Pauses and slower ramp rates were added to allow the BaO_2 and Tl_2O_3 to evolve oxygen, but these proved unnecessary.

3.2 Salt Sealing

The first salt-based technique tried, which used a lake of salt, sealed the thallium in very effectively. However, the salt contaminated the reactants and prevented $Tl_2Ba_2CuO_{6\pm\delta}$ from forming (see Subsection 2.4.1). The salt technique was not immediately abandoned, but it did have to be significantly modified.

When a much smaller amount of salt was used ($\sim$0.4 g), the melt was not contaminated. However, the sealing was poorer, and 20-50% of the thallium escaped, depending on such conditions as the maximum temperature, the time taken for growth (1$\sim$2 h) and the initial thallium content of the crucible's charge.

3.3 Gold Sealing

The simple replacement of salt with gold, coupled with the addition of a gold lid, improved the sealing slightly – with mixtures of Tl : Ba : Cu of 3 : 2 : 2, about 30 – 50% of the thallium was lost. The use of salt combined with gold provided a negligible improvement.

When the alloy was used with gold to help seal the crucible, only 10 – 25% of the thallium was lost after a prolonged growth ($>$55 h), and a few Tl-2201 crystals were obtained, with T_c's ranging from 5 – 90K. The gold coin corroded slightly, losing around 3 mg of mass per growth run. It is perhaps worth noting that while Hastelloy X is designed for use in jet engines, it does not fare as well in hot oxygen,
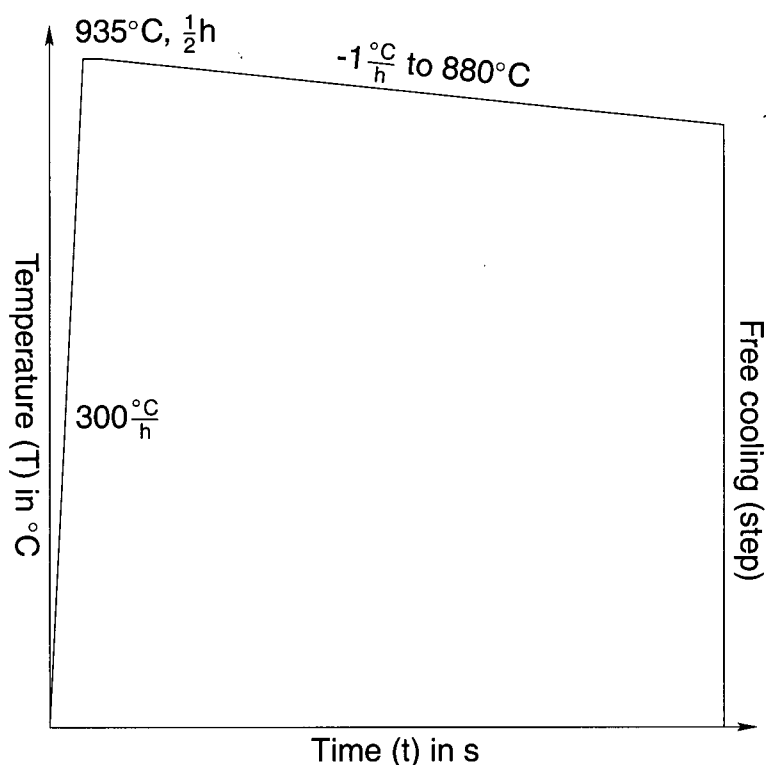
Figure 3.2: An example of a furnace program – this was the furnace program used when the alloy was inaugurated.

leading to concerns that it pollutes the furnace with nickel-containing vapours. The contents of the crucible should be adequately isolated from this thanks both to the sealing and the slight excess pressure in the crucible during growth.

3.4 Carbon Dioxide

Each group to have successfully grown Tl-2201 crystals used BaO_2 as an ingredient, in place of $BaCO_3$, but none have explained their reasoning. We found that the presence of carbon all but precluded the formation of Tl-2201. Magnetization measurements on solidified flux showed only very weak diamagnetism when carbonates had been present. This startling result can be explained by oxycarbonate formation. The presence of carbon would be difficult to detect by XRD or especially any EDX or EPMA-like system, where graphite is used to ground the

sample's surface.

A substantial number of stable Tl-Ba-Cu oxycarbonates are known to exist[28], some with structures similar to Tl-2201, but with Tl and Cu partially or totally replaced by carbon (e.g. $TlSr_{4-x}Ba_xCu_2CO_3O_7$). The presence of carbon, therefore, changes the phase diagram totally.

The solution to the oxycarbonate problem seems clear: carbon must be excluded from the reactants. This is easier said than done. As was observed in Subsection 1.3.2, BaO_2 is essentially unavailable in purities over 95%, and contains a few % $BaCO_3$. The solution, then, must lie in using binary reactants, such as $BaCuO_2$ or $Tl_2Ba_2O_5$, in place of BaO_2 or $BaCO_3$.

Thallium barium oxide powders are difficult to make, thanks to the thallium's vapour pressure, but there's an additional nuisance here: several thallium barium oxycarbonates are stable. We thus chose barium cuprate to replace BaO_2.

$BaCuO_2$ was prepared from CuO and $BaCO_3$ by repeated calcining in an Al_2O_3 tray at 850°C, after which a final calcining step at 850°C for 2 weeks in flowing O_2 removed nearly all remaining carbonate. It was noticed, however, that the powder was reacting with the carbon dioxide in air (see Figure 3.3). It must be stored in airtight containers and handled rapidly, to minimize its exposure to air.

A simpler procedure was devised to synthesize $BaCuO_2$ with a minimal carbon content. CuO and $Ba(NO_3)_2$ (Alfa Æsar, 99.999% pure), which is stable in air, were ground together in an agate mortar and pestle. NO_2 gas is evolved at 590°C, where the barium nitrate melts. The temperature program passed very slowly through this transition, and only small quantities were placed in each vessel, as the evolution of NO_2 is quite rapid at that transition. It was determined that the mixture becomes a molten slurry at the melting point, with violent boiling. The mixture was further heated to 850°C, to ensure complete reaction. NO_2 gas is corrosive only when it comes into contact with water or water vapour, so the interior of the furnace

Figure 3.3: $BaCuO_2$ ceramic after oxygen anneal to remove CO_2 and subsequent brief storage at room temperature. Upon removal from the furnace, all pieces were black. The oxygen was flowing from right to left, so the pieces to the right had nearly all carbon dioxide removed, while those downstream, to the left, did not. For CO_2 to re-enter the ceramic at right, the ceramic had to decompose.

used, which is extremely dry, should be unmolested. There are concerns, however, about nearby apparatus, the exterior of the furnace, and the exhaust vents over the furnace.

While weighing the resulting pure $BaCuO_2$ powder on the analytical balance, the mass could be observed to increase steadily, as CO_2 was absorbed from the air. The powder must therefore be stored either under vacuum or in a small, airtight container, to limit the amount of CO_2 it can absorb. All subsequent handling, mixing and weighing steps were performed as quickly as possible, as they were performed in air.

A crystal growth run using $BaCuO_2$ powder prepared in this manner in combination with the alloy weight to improve the gold seal was particularly successful, with the major phase being crystalline Tl-2201. Several crystals extracted from this batch had surfaces suitable for microwave measurements, and all had T_c's around 6K, several Kelvins wide.

Figure 3.4: Optical micrograph of an as-grown 90K sample.

3.5 Characterization

The first growth run using the alloy weight produced several samples with T_c's around 90K and typical sizes of $\frac{1}{2} \times \frac{1}{2}$ mm^2 to 1×1 mm^2. An optical micrograph of a characteristic such sample is shown in Figure 3.4. This sample produced a large diamagnetic signal when measured in our Quantum Design SQUID magnetometer, but its surfaces are clearly not microwave-quality. Indeed, its few shiny faces and bulk superconductivity are consistent with the sample being largely polycrystalline Tl-2201.

While early XRD scans of the 90K samples typically found clear evidence of c-axis oriented Tl-2201, optical micrographs such as Figure 3.4 suggested that these samples might merely be crystallites on polycrystalline $Tl_2Ba_2CuO_{6\pm\delta}$. A (0 0 10) rocking curve (Figure 3.5) of the above sample found multiple weak peaks, only twice as intense as the background, supporting the polycrystalline view. The wide
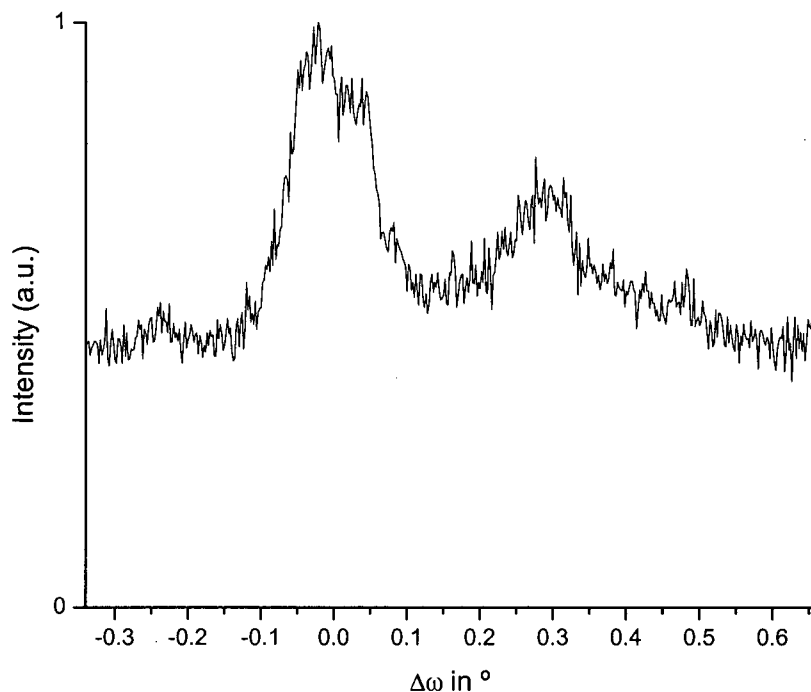
Figure 3.5: (0 0 10) rocking curve for the 90K sample shown in Figure 3.4.

slits required to observe these peaks may have limited their widths, but very small crystallites would be expected to exhibit very narrow rocking curves. By optical micrograph, this sample was characteristic of those from its growth run, but this does not imply that all of those were as poor as this rocking curve suggests.

The residual transition at 8K in Figure 3.6 may reflect a different region of the sample, coexistence of tetragonal and orthorhombic phases, strain from thermal contraction, or any number of other effects – in such a sample, a second transition is neither a surprise nor a concern.

A subsequent growth run described in Section 3.4 produced crystals with T_c's of $\sim$6K, several Kelvins wide, thin plates with typical sizes of 1×1 mm^2. An optical micrograph of one such crystal is shown in Figure 3.7, and its SQUID magnetization curve is provided in Figure 3.8. It is worth noting that, unlike YBa$_2$Cu$_3$O$_{6+\delta}$, Tl$_2$Ba$_2$CuO$_{6\pm\delta}$ does not appear to be predisposed toward cleaving along (1 0 0) and (0 1 0) directions.
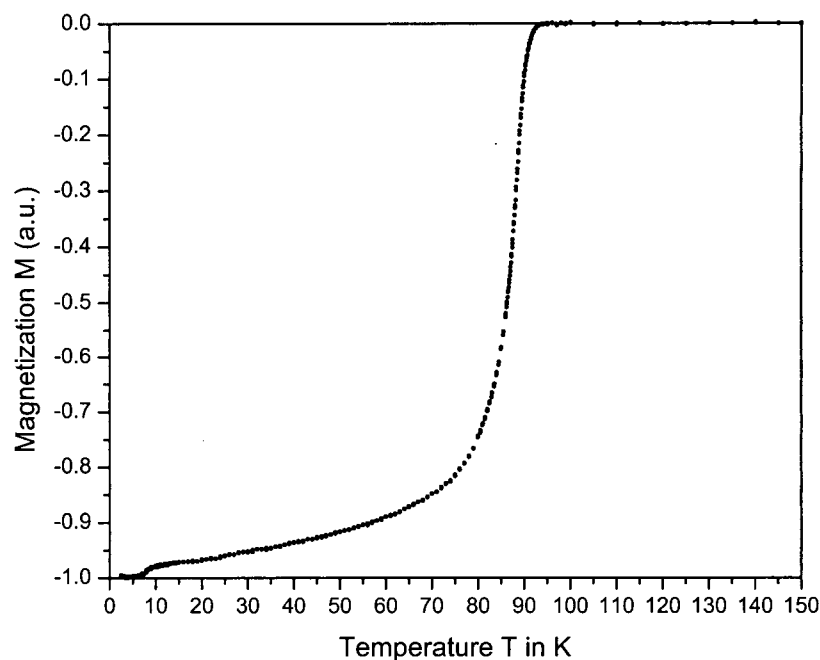
Figure 3.6: Magnetization curve for the 90K sample shown in Figure 3.4. Note the residual 8K transition.

As was the case for the 90K sample, this crystal's (0 0 10) rocking curve (Figure 3.9) has several peaks, probably due to extra domains. The peaks are $\lesssim 0.04°$ wide, and are strong. The apparent presence of multiple domains in this crystal is disappointing, but it reinforces the fact that this is a very early crystal and the growth technique still requires much optimization.

Figure 3.10 shows a $\theta/2\theta$ scan through the 5K crystal's (0 0 N) reflections. The c-axis lattice parameter was found to be 23.143(2) Å, which is roughly consistent with previously reported values for low-T_c Tl-2201 (for example, 23.1332(9) Å for a $T_{c(onset)}$ = 12.4K crystal[19], and 23.1369(5) Å for a nonsuperconducting ceramic sample[8]). For comparison, c at optimal doping is around 23.24 Å[18].
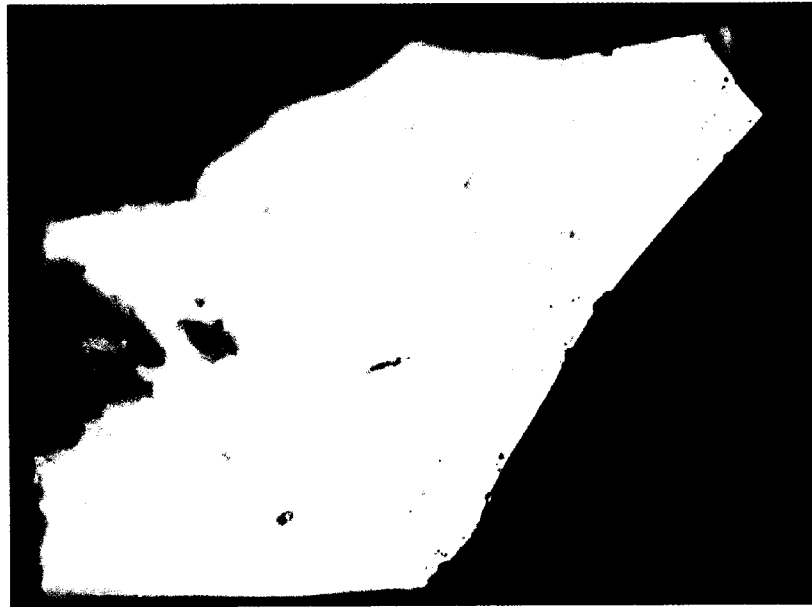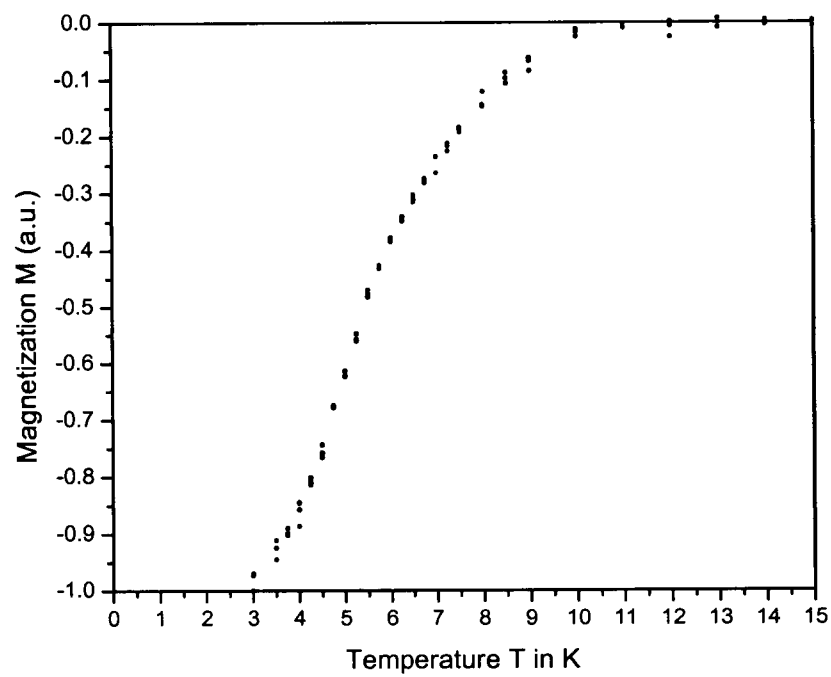
Figure 3.7: Optical micrograph of an as-grown 5K crystal.

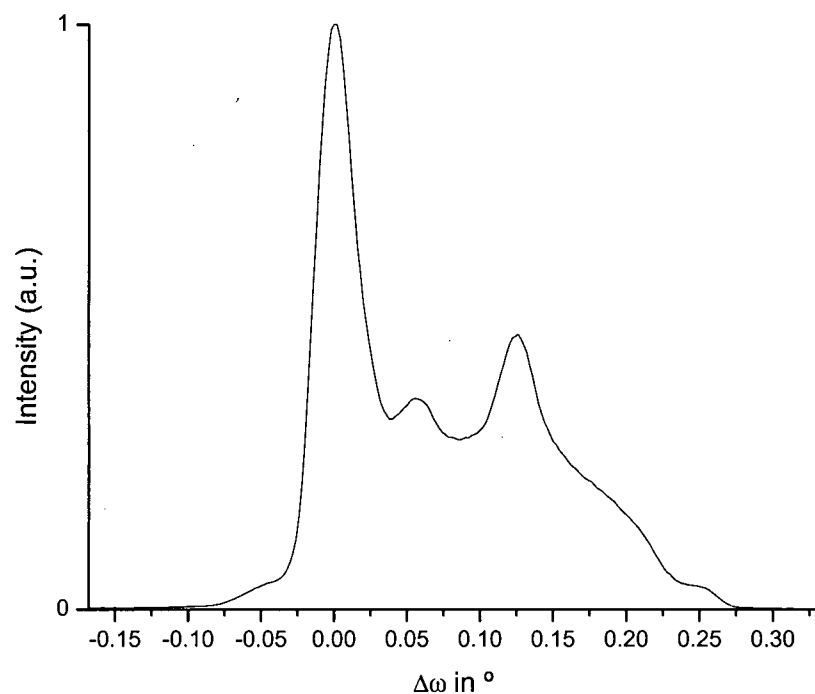Figure 3.8: Magnetization curve for the T_c = 5K crystal shown in Figure 3.7.

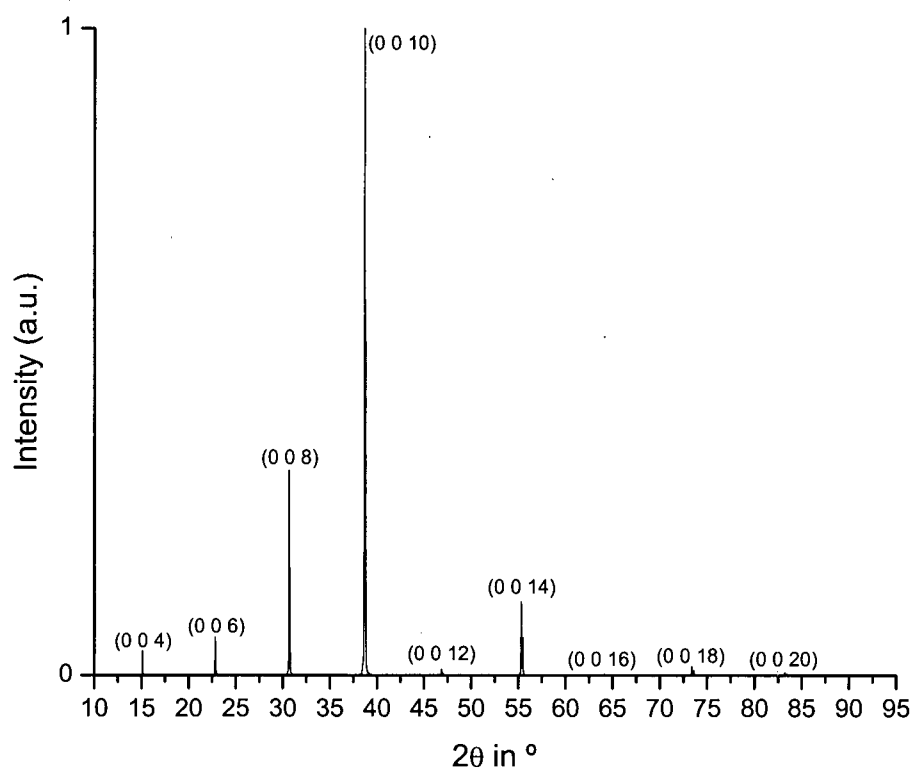Figure 3.9: (0 0 10) rocking curve for the 5K crystal shown in Figure 3.7.

Figure 3.10: c axis (or (0 0 N)) scan for the 5K crystal. Its lattice parameter was found to be $c = 23.143(2)$ Å.

Chapter 4

Conclusions

Single crystals of Tl-2201 have been grown using a copper-rich self-flux method. As-grown T_c's varied from 5K to 90K and were several Kelvins wide, but growth and doping have not yet been controlled. Samples with T_c's around 90K have thus far all been largely polycrystalline, while the T_c = 5K sample analyzed had several domains. The c-axis lattice parameter found for the 5K crystal, 23.143(2) Å, is comparable to those found on previous low-T_c Tl-2201 samples.

A second transition in the 90K sample, at 8K, is likely due to inhomogeneity.

It was found to be crucial for successful growth of Tl-2201 crystals that the thallium vapours be contained and that carbon be excluded. The effects of other potential impurities have not yet been investigated.

Although crystals of $Tl_2Ba_2CuO_{6\pm\delta}$ have been grown, the tasks of optimizing their growth and characterizing them have barely begun. The crystals may be more readily grown under pressure, to better contain the thallium oxide vapours. A method should be devised for removing the flux from the crystals before it freezes, and temperature gradients may aid crystal growth. The furnace program and initial compositions have not been optimized, and the sealing system could be improved. The carbonate concentration can still be lowered, and alternatives to $BaCO_3$ more fully explored. Alternative crucible materials, such as $BaZrO_3$ and gold, should be tested, and the impurity levels due to crucible materials (currently Au and Al) must be measured and minimized.

Annealing was not covered in this thesis, but will be required, to set the oxy-

gen content precisely and make the crystals more homogeneous. With very little information available on this at present, a thorough doping study will require considerable effort, particularly due to the volatility of thallium. Once the purity, doping and possible homogeneity issues have been resolved, it will be important to determine exactly what is substituting for thallium in our crystals (copper, carbon, vacancies, or some other atom currently above suspicion), if anything, and to what extent. We will also need to determine whether our crystals are orthorhombic or tetragonal, and attempt to grow crystals of the other phase.

Once we have control over Tl-2201, it would likely be worthwhile to check whether crystals of Tl-1201 ($TlBa_2CuO_5$) can be grown at or near atmospheric pressure. This compound is single-layer, tetragonal, overdoped, and possibly undopable. It has an even simpler unit cell than $Tl_2Ba_2CuO_{6\pm\delta}$, and resists the substitution of Cu for Tl. Whether its oxygen content may be varied is not clear – studies of this compound thus far have been tainted with doubts over the possible inclusion of Tl-2201 as an impurity phase. The Tl-Ba-Cu oxide phase diagram has not been mapped out, so Tl-1201 crystal growth cannot be ruled out. A related project would be to map out the entire Tl-Ba-Cu oxide phase diagram, determining where the tie lines are. Aside from being required in the search for Tl-1201, this could allow us to grow crystals of both orthorhombic and tetragonal Tl-2201, or to find more favourable growth compositions.

Once Tl-2201's quality and doping are controlled, magnetization, resistivity and microwave surface resistance measurements should be performed by our group, to compare the overdoped and underdoped sides of the phase diagram. Our collaborators, too, will be interested in Tl-2201. The Fermi surface mapping techniques mentioned earlier should be applied, as should ARPES. The crystals should be fully characterized across their entire doping range.

References

[1] J. G. Bednorz and K. A. Müller, Z. Physik B **64**, 189 (1986).

[2] A. Erb, E. Walker, and R. Flükiger, Physica C **245**, 245 (1995).

[3] R. Liang, D. A. Bonn, and W. N. Hardy, Physica C **304**, 105 (1998).

[4] R. Liang, D. A. Bonn, and W. N. Hardy, Physica C **236**, 57 (2000).

[5] P. Manca *et al.*, Phys. Rev. B **63**, 134512 (2001).

[6] Z. Z. Sheng and A. M. Hermann, Nature **332**, 55 (1988).

[7] Y. Shimakawa, Y. Kubo, T. Manako, and H. Igarashi, Phys. Rev. B **40**, 11400 (1989).

[8] Y. Shimakawa, Y. Kubo, T. Manako, and H. Igarashi, Phys. Rev. B **42**, 10165 (1990).

[9] J. B. Parise, C. C. Torardi, M. A. Subramanian, J. Gopalakrishnan, and A. W. Sleight, Physica C **159**, 239 (1989).

[10] N. N. Kolesnikov *et al.*, Physica C **242**, 385 (1995).

[11] A. Tyler, *An Investigation into the Magnetotransport Properties of Layered Superconducting Perovskites*, Ph.D. thesis, University of Cambridge, 1998.

[12] Y. Shimakawa, Physica C **204**, 247 (1993).

[13] N. N. Kolesnikov *et al.*, Physica C **195**, 219 (1992).

[14] O. M. Vyasilev, N. N. Kolesnikov, M. P. Kulakov, and I. F. Schegolev, Physica C **199**, 50 (1992).

[15] J. L. Jorda *et al.*, Physica C **205**, 177 (1993).

[16] R. C. Weast, *CRC Handbook of Chemistry and Physics*, 70th ed. (CRC Press, 1989).

[17] T. Manako, Y. Kubo, and Y. Shimakawa, Phys. Rev. B **46**, 11019 (1992).

[18] C. C. Torardi *et al.*, Phys. Rev. B **38**, 225 (1988).

[19] R. S. Liu *et al.*, Physica C **198**, 203 (1992).

[20] M. Hasegawa, Y. Matsushita, Y. Iye, and H. Takei, Physica C **231**, 161 (1994).

[21] M. Hasegawa, H. Takei, K. Izawa, and Y. Matsuda, J. Cryst. Growth **229**, 401 (2001).

[22] C. Opagiste *et al.*, Physica C **213**, 17 (1993).

[23] C. Opagiste *et al.*, J. Alloy Compd. **195**, 47 (1993).

[24] T. K. Jondo, R. Abraham, M. T. Cohen-Adad, and J.-L. Jorda, J. Alloy Compd. **186**, 347 (1992).

[25] R. J. Ormeno, A. Sibley, C. E. Gough, S. Sebastien, and I. R. Fisher, Phys. Rev. Lett. **88**, 047005 (2002).

[26] C. Petrovic *et al.*, Europhys. Lett. **53**, 354 (2001).

[27] P. Chartrand and A. D. Pelton, Canadian Metallurgical Quarterly **40**, 13 (2000), and references therein.

[28] B. Raveau, C. Michel, B. Mercey, J. F. Hamet, and M. Hervieu, J. Alloy Compd. **229**, 134 (1995), and references therein.

Appendix A

Preparation and Growth Procedures

This Appendix describes the techniques employed in the preparation of a common precursor to our research (blondie bars). Much like espresso, this substance is extremely helpful in the continuation of our fundamental research on superconductors.

Carefully dispensed quantities of sucrose (240 mL) and a vegetable fat-based table spread (120 mL) were intimately mixed in a large translucent polymeric reaction vessel, at which point two large, deshelled chicken eggs were similarly mixed in. In a smaller reaction vessel, a solid solution was formed of an unbleached, powdered gluten source (360 mL) and baking powder (2.5 mL). This solid solution was gradually added, along with dihydrogen monoxide (30 mL) and vanilla (2.5 mL), to the original solution. Finally, 90 – 120 mL of chocolate chips were added, forming a viscous suspension with a characteristic off-white colour.

This viscous suspension was decanted into a silicon dioxide tray with interior dimensions 13" × 9" and a wall thickness of roughly 3 mm, upon which had previously been deposited a thin film of the vegetable-based substance mentioned above. The mixture was calcined for 20 minutes at 175°C in a standard low-temperature muffle furnace, then allowed to cool freely to room temperature. It was observed that the sample's characteristic off-white colour had darkened to beige.